CONSTRUCTION OF AN RF-BAND TEST FIXTURE MODEL USING 3-D FIELD SIMULATOR

KiHyuk Kim, GyoungBum Kim, Seung Yong Cha, and SungWoo Hwang
Department of Electronics & Computer Engineering
Korea University
Anam, Sungbuk
Seoul 136-701, Korea

Received 2 September 2005

ABSTRACT: *For design and characterization of packaged RF-band transistor amplifiers, test fixtures consisting of coaxial connectors and planar-type transmission lines are frequently used. We present a method of extracting 3D field simulation parameters of these test fixtures and demonstrate that a circuit model of the test fixtures can be constructed by pure 3D field simulation using the extracted material constants. The developed circuit model predicts measurement results within 0.5 dB.*
 Microwave Opt Technol Lett 48: 498–500, 2006; Published online in Wiley InterScience (www.interscience.wiley.com). DOI 10.1002/mop.21390

Key words: *3D field simulation; test fixtures; dielectric constant; packaging*

1. INTRODUCTION

Three-dimensional (3D) field simulation of a whole RF circuit would be an ideal way of predicting the performance, since complete electromagnetic interaction between components is automatically included in the simulation results [1]. The field simulation of active components is not yet realistic, but it becomes quite possible to obtain the circuit parameters of passive test fixtures. The parameters of the 3D simulation are the effective dielectric constant of materials, the dimensions of simulated structures, the boundary conditions for problem regions, the convergence criterions, and so on. Among them, the most important parameter is the effective dielectric constant of the used materials. For example, the dielectric constant of typical FR4 substrates is in the range of 4.2 to 4.9 [2]. This uncertainty could result in $>$50% variation of the characteristic impedance and the S-parameters response of the test fixtures [3].

The usual test fixtures consist of coaxial connectors and planar-type transmission lines. A conventional way of modeling them has been the series of high-cost RF probe measurements and de-embeddings of circuit parameters [4]. Furthermore, such circuit modeling necessarily includes the transition region between the coaxial connector and the transmission line. It is extremely difficult to obtain accurate de-embedding of the transition model parameters.

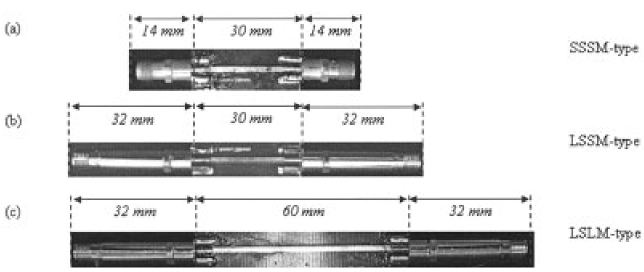

Figure 1 Designed test jigs: (a) SSSM-type; (b) LSSM-type; (c) LSLM-type

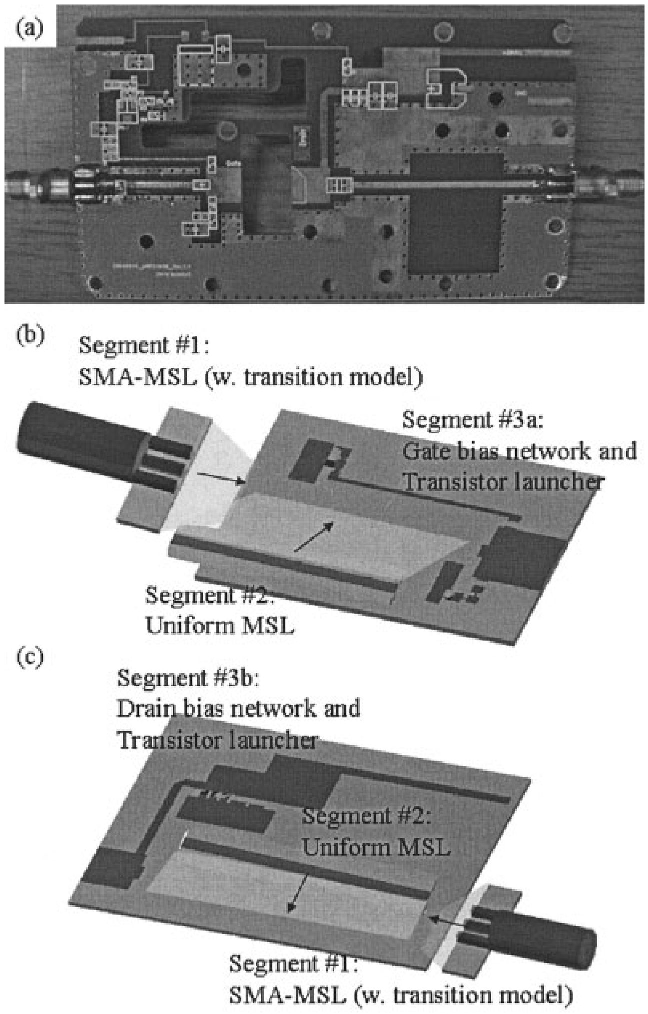

Figure 2 Designed test fixtures for the LDMOS transistor amplifier: (a) photography; (b) segmented 3D field simulation model of the left-side of the test fixtures; (c) segmented 3D field simulation model of the right-side of the test fixtures

In this paper, we first show a unique way of separately measuring the dielectric constants of the test fixtures. The main idea is to design the test jigs, which have the same type of transition regions and differ only in the electrical length of the uniform regions. The effective dielectric constants of each region can be extracted from the difference in the measured propagation delays of the test jigs, and the consideration of the cumbersome transition region can be avoided. The 3D field simulation of an RF amplifier test fixtures using the obtained effective dielectric constant provides the multiport S-parameters. Here, the field simulation automatically handles the characteristic of the transition region. The obtained multiport S-parameters are used in the circuit simulation with active components and the results of the circuit simulation are in reasonable agreement with measured results.

2. EXTRACTION OF EFFECTIVE DIELECTRIC CONSTANT OF TEST FIXTURES

Figures 1(a)–1(c) show three types of test jigs. The short-SMA short microstrip line (SSSM)-type test jig has a 30-mm-long FR4 microstrip line between 14-mm-long standard SMA connectors. The long-SMA short-microstrip line (LSSM)-type test jig has a 30-mm-long FR4 microstrip line between 32-mm-long SMA connectors. The long-SMA long-microstrip line (LSLM)-type test jig

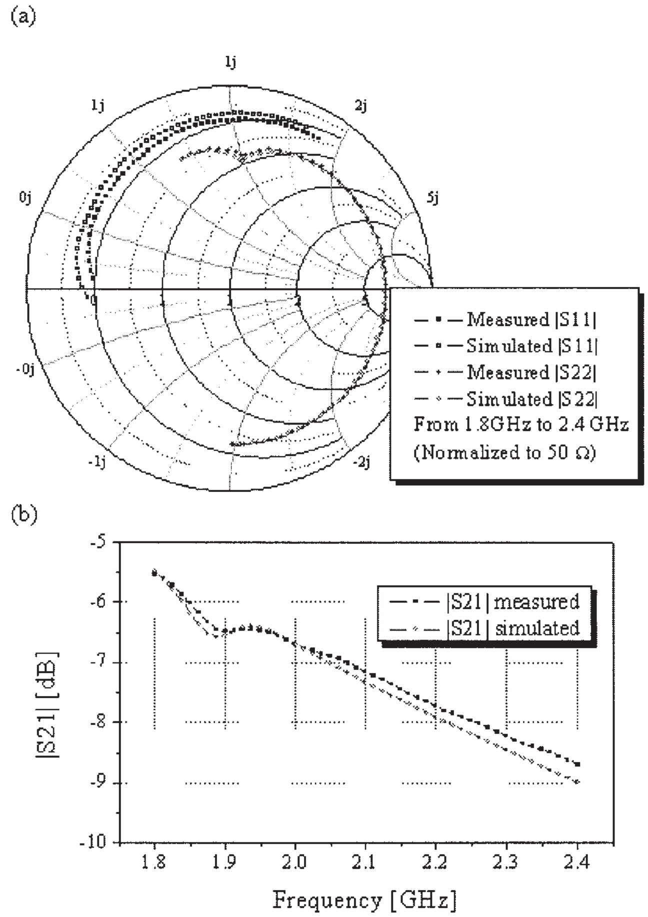

Figure 3 *S*-parameters responses of the through-connected left- and right-side of the test fixtures: (a) S_{11} and S_{22} responses; (b) $|S_{21}|$ responses

has a 60-mm-long FR4 microstrip line between 32-mm-long SMA connectors.

The effective dielectric constant of the SMA connector is obtained from the electrical-delay difference between the SSSM-type and LSSM-type, and the effective dielectric constant of the microstrip line is obtained from the electrical-delay difference between the LSSM-type and LSLM-type test jigs. By comparing the measurement results from the test jigs of the same type but with different physical lengths of a particular uniform regions, the propagation velocity of the uniform region is obtained. The key point of this idea is that the propagation delay, which is obtained, does not depend on the details of the transition regions that are inevitably included in the test jigs. Therefore, the effective dielectric constants of each uniform region are calculated from the measured propagation-delay differences. Eq. (1) shows the relationship between the difference in the physical length and the effective dielectric constant:

$$v = \frac{\Delta l}{\Delta t} = \frac{c}{\sqrt{\varepsilon_{eff}}} \Rightarrow \varepsilon_{eff} = \left(\frac{\Delta t}{\Delta l}c\right)^2, \tag{1}$$

where Δl is the difference in the physical length, Δt is the difference in the propagation times, c is equal to the speed of light, and ε_{eff} is the effective dielectric constant of the uniform regions. The electric delays are measured with the electrical delay modification function of the HP 8753ES VNA. The measured electrical-delay values of the SSSM-, LSSM-, and LSLM-type test jigs are 0.161, 0.316, and 0.493 ns, respectively. The extracted effective dielectric constant of SMA connector and that of the microstrip line are calculated to be 1.667 and 3.182, respectively. Notice that the dielectric constant of the microstrip line is a function of the frequency when the frequency is larger than 3 GHz (dispersion effect) [5]. In this case, a modified form of Eq. (1), including frequency-dependent dielectric constant, can be used.

3. 3D FIELD SIMULATION MODEL OF TEST FIXTURES

Figure 2(a) shows the fabricated test fixtures for a RF-band LD-MOS transistor amplifier. The segmentation of the test fixtures is performed for efficient 3D simulations. Figures 2(b) and 2(c) show the corresponding segmented 3D field simulation models. The input-side and output-side test fixtures are segmented into three sections, respectively. They are consisted of the SMA-to-microstrip line section, including both the nonuniform region and the uniform SMA region, the uniform microstrip line section, and the bias network section that includes the transistor launcher.

4. EXPERIMENTAL VERIFICATION

Figures 3(a) and 3(b) show the *S*-parameters of the through-connected input-side and output-side test fixtures. The simulated results can predict the measured characteristics of the test fixtures within 0.5-dB accuracy in the frequency range from 1.8 to 2.4 GHz.

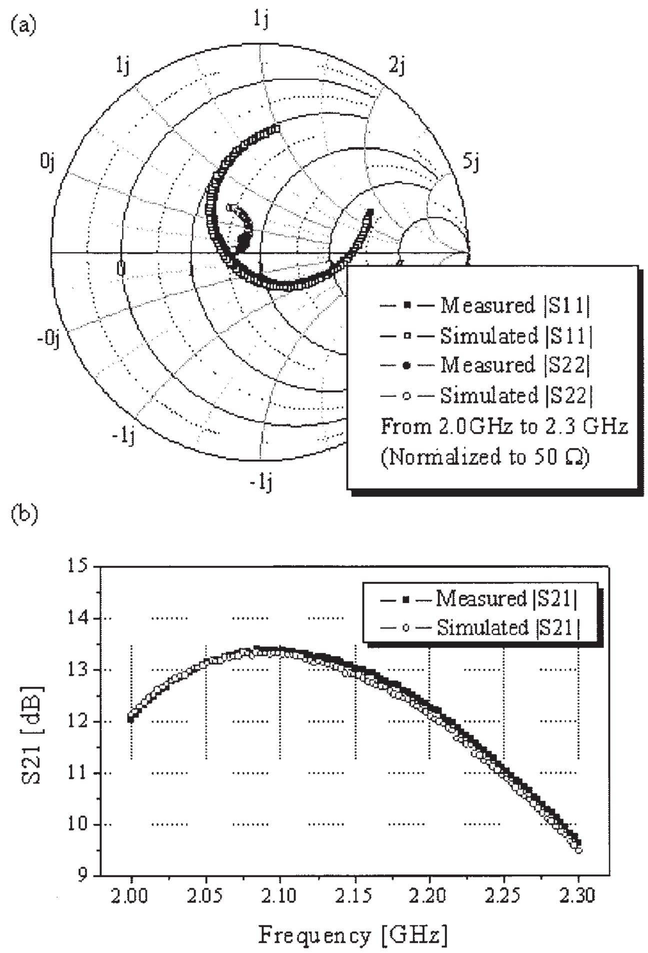

Figure 4 *S*-parameter responses of the impedance-matched transistor amplifier embedded in the test fixtures: (a) S_{11} and S_{22} responses; (b) $|S_{21}|$ responses

The intrinsic characteristics of LDMOS transistor amplifier can be extracted by removing the simulated characteristics of the input side and output side of test fixtures from the overall measured characteristics. In addition, impedance-matching networks are designed with these extracted S-parameters of the LDMOS transistor amplifier. The transistor used in this work is an MRF21030 LDMOS 30W transistor provided by Freescale Semiconductor, Inc., and biased such that I_{DS_DQ} is equal to 200 mA. Figures 4(a) and 4(b) show the measured and simulated S-parameters of the impedance matched transistor amplifier in the frequency range from 2.0 to 2.3 GHz. The maximum deviations of the measured $|S_{11}|$, $|S_{21}|$, and $|S_{22}|$ from the simulated $|S_{11}|$, $|S_{21}|$, and $|S_{22}|$ are 0.66, 0.17, and 0.13 dB, respectively. The simulated characteristics of impedance matching blocks can accurately predict the measured ones, as shown in Figures 4(a) and 4(b).

5. CONCLUSION

In this paper, we have presented a method of extracting 3D field simulation parameters of RF-band transistor amplifier test fixtures and demonstrated that a circuit model of the test fixtures can be constructed via pure 3D field simulation using the extracted material constants. The developed circuit model predicts measurement results within 0.5 dB.

REFERENCES

1. H. Liang, J. Laskar, H. Barnes, and D. Estreich, Design and optimization for coaxial-to-microstrip transition on multilayer-substrate, IEEE MTT-S Int Microwave Symp Dig, Pheonix, AZ (2001), 1915–1918.
2. R.W. Rhea, Designing a low-noise VCO on FR4, RF Design 9 (1999), 72–77.
3. E. Bogatin, A closed-form analytical model for the electrical properties of microstrip interconnects, IEEE Trans Compon Packaging and Manufac Technol 13 (1990), 258–266.
4. In-fixtures measurements using vector network analyzers, Agilent Technologies Application Notes 1297–1299, 1999.
5. B.C. Wadell, Transmission line design handbook, Artech House, Boston, 1991.

ULTRA-WIDEBAND SQUARE-SLOT ANTENNA

Horng-Dean Chen,[1] Jin-Sen Chen,[2] and Jui-Ni Li[1]

[1] Department of Optoelectronics and Communication Engineering
National Kaohsiung Normal University
Kaohsiung 824, Taiwan
[2] Department of Electronic Engineering
Cheng Shiu University
Kaohsiung 833, Taiwan

Received 31 August 2005

ABSTRACT: *A simple square-slot antenna capable of providing a very wide impedance bandwidth of larger than 9 GHz is presented. The ultra-wideband operation for the proposed antenna is realized by using a novel feeding mechanism of loading an offset rectangular stub at the end of the microstrip feed line. With the proper offset distance of rectangular stub chosen, the proposed antenna can operate in the 2.78–12.02-GHz frequency range and covers the UWB operating bandwidth of 3.1–10.6 GHz. The antenna radiation patterns at 3, 5.3, 7.9, and 10 GHz are also presented.* © 2006 Wiley Periodicals, Inc. Microwave Opt Technol Lett 48: 500–502, 2006; Published online in Wiley InterScience (www.interscience.wiley.com). DOI 10.1002/mop.21391

Key words: *slot antenna; ultra-wideband antenna*

1. INTRODUCTION

Recent interest in the development of ultra-wideband (UWB) communication systems has prompted the study of UWB antennas. Printed wide-slot antennas are promising candidates for UWB systems because of their broadband characteristics. At present, several UWB designs of wide-slot antennas have been reported, including the uses of a circular slot with elliptic or rectangular microstrip-fed structures [1–3], a volcano-smoke slot with a CPW-fed structure [4], and a tapered-slot-fed annular slot [5]. However, it is noted that among wide-slot antennas with various shapes, the square-slot antenna is simple in geometry, but it has the drawback of providing a relatively smaller impedance bandwidth and has rarely been researched with the goal of UWB operation. Therefore, efforts to further improve the bandwidth of the square-slot antenna are needed for applications in UWB systems.

In this paper, we propose a novel feed structure for the square-slot antenna that can achieve a good impedance matching over a much wider frequency range. The feed structure is composed of an offset rectangular stub connected at the end of the microstrip feed line. The offset of the rectangular stub has a predominant role in achieving the UWB performance. Details of the antenna design are described, and experimental results of the proposed antenna are presented and discussed.

2. ANTENNA DESIGN

Figure 1 shows the geometry of the proposed UWB square slot antenna. The square slot (size 31×31 mm^2) is etched on an FR4 microwave substrate of thickness 0.8 mm and relatively permittivity 4.4. A 50Ω microstrip feed line with an offset rectangular stub (size $L \times W$) is printed on the back side of the microwave substrate. Here, the centerline of the rectangular stub is placed on an offset distance of d from the centerline (Y-axis) of the feed line. The spacing between the rectangular stub and edge of the ground plane is S.

For a square slot antenna with a conventional rectangular microstrip-fed structure ($d = 0$ in Fig. 1), the dimensions (L and W) of the rectangular stub and the spacing S are optimized in order to achieve the widest possible bandwidth operation. But the resultant antenna provides inadequate coverage at the UWB operating bandwidth of 3.1–10.6 GHz. However, for the proposed antenna with an offset rectangular microstrip-fed structure, the offset distance of the rectangular stub is found to have a great effect on

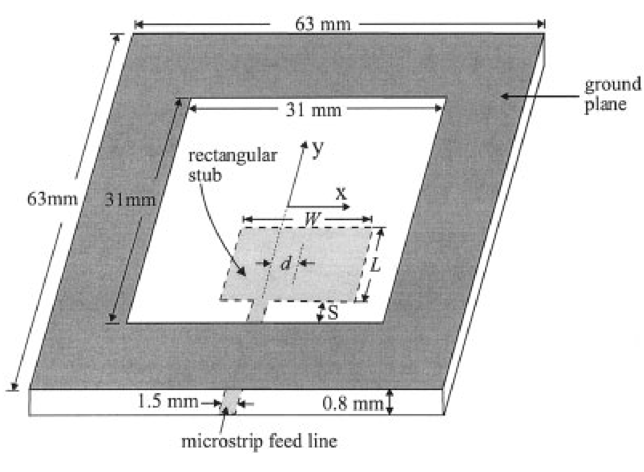

Figure 1 Geometry of the proposed UWB square-slot antenna fed by an offset rectangular microstrip line